Journal of Solid State Chemistry **163,** 506–512 (2002)
doi:10.1006/jssc.2001.9438, available online at http://www.idealibrary.com on IDEAL®

Comprehensive Study of Third-Order Nonlinear Tungstates: Relationship between Structural and Vibrational Properties in Raman Shifters

E. Gallucci, C. Goutaudier, F. Bourgeois, G. Boulon, and M. Th. Cohen-Adad

Laboratoire de Physico-Chimie des Matériaux Luminescents, UMR CNRS 5620-Université Claude Bernard Lyon 1, 43, Bd du 11 novembre 1918, 69622 Villeurbanne cedex, France

Received July 24, 2001; in revised form October 17, 2001; accepted October 26, 2001

Although tungstates are now well known as laser Raman shifters, their physicochemical properties (especially the vibrational ones) were not often studied. We have carried out a comprehensive and systematic study of tungstate Raman spectra, thanks to which, structural and vibrational properties could be correlated. It was shown that the Raman scattering characteristics of these compounds are directed by simple physical chemistry parameters. They change logically with easy interpolation. The optimization of the search for tungstates as new efficient Raman shifters was realized through a figure of merit: a map where the Raman frequency is described versus a normalized parameter representative of the Raman gain. © 2002 Elsevier Science (USA)

INTRODUCTION

During the past 20 years, a high interest in the search for new efficient solid state laser sources has been observed and many works have been published. Particularly, numerous attempts were carried out to prepare lasers emitting around 1.55 μm (1) (eye-safe domain) but also in the whole near-IR spectral domain (2). One way to generate such wavelengths is to use third-order nonlinear materials (Raman shifters) which are able to convert usual commercial laser frequencies (such as Nd-YAG), through Raman scattering (3).

Tungstates are promising Raman shifters as the tungsten–oxygen bonds exhibit high internal vibration frequencies. They are thus highly studied but, for many years, the only published data essentially dealt with their luminescence characterization as either pure or doped materials. Today more attention is paid to the material properties but a lack of correlation between the physicochemical and Raman properties is observed although some unsuccessful attempts were made to correlate the W–O stretching mode wavenumber with W–O bond lengths in tungstates (4). But such attempts present the opportunity to evidence the distortion of W tetrahedra or octahedra when equivalent vibrational modes are compared (4).

The purpose of the present work is to fill this lack of information by determining the parameters that control tungstates' Raman properties. The efficiency of a Raman shifter is dependent on its frequency shift and on its band integral involving the peak intensity and the band width. By analogy with the important works with vibrational spectroscopy that were carried out on carbonate and silicate compounds (5) (close to tungstates from a chemical bonding point of view), correlation between Raman properties and simple parameters such as element mass, ionic radius, etc. have been investigated.

We thus have carried out a systematic study of the Raman properties of the three major tungstate families: the mono-, di-, and tritungstates with formula DWO_4, $AL(WO_4)_2$, and $L_2(WO_4)_3$ where A, D, and L are monovalent, divalent, and trivalent cations, respectively. Raman shift and peak integral evolutions of these compounds were first considered according to simple intrinsic physical chemistry parameters of A, D and L. A graph allowing one to estimate these tungstates' application power in third-order nonlinear optics has been proposed.

EXPERIMENTALS

All compounds (listed in Table 1) were prepared by solid state reaction at high temperature between reagents in required proportions. Thermal treatments were achieved on the basis of DTA–TG results obtained with a SETARAM TAG 24 thermoanalyzer (measurements at 10 K/mn, in platinum crucible, under oxygen flow). Phases' purity was checked through XRD powder patterns using a PHILIPS PW3710 diffractometer at $\lambda = K\alpha\text{Cu}$. Powder Raman measurements were performed using a DILOR XY spectrophotometer under a 514 nm laser excitation (argon). Spectra were analyzed through factor group analysis (FGA).

0022-4596/02 $35.00

TABLE 1
Raman Shift Frequency of Some Studied Tungstates

Compound	Wavelength (cm^{-1})	Compound	Wavelength (cm^{-1})	Compound	Wavelength (cm^{-1})
$BaWO_4$	960	$NaAl(WO_4)_2$	1013	$RbSc(WO_4)_2$	1009
$SrWO_4$	921	$NaY(WO_4)_2$	918	$RbIn(WO_4)_2$	1008
$PbWO_4$	904	$NaGd(WO_4)_2$	916	$RbGd(WO_4)_2$	901
$CaWO_4$	910	$NaBi(WO_4)_2$	876		
$ZnWO_4$	907	$NaIn(WO_4)_2$	974 (10)		
$LiAl(WO_4)_2$	1014	$KSc(WO_4)_2$	1009	$Al_2(WO_4)_3$	1049
$LiSc(WO_4)_2$	990	$KY(WO_4)_2$	905	$Sc_2(WO_4)_3$	1024
$LiLu(WO_4)_2$	918	$KGd(WO_4)_2$	902	$Gd_2(WO_4)_3$	948
$LiY(WO_4)_2$	914	$KBi(WO_4)_2$	874	$Ce_2(WO_4)_3$	944
$LiBi(WO_4)_2$	891	$KIn(WO_4)_2$	975 (10)	$La_2(WO_4)_3$	945

Note: All compounds presented herein have been prepared and investigated in our lab (14–16).

LITERATURE DATA

From a structural point of view, the comparison of mono-, di-, and tritungstates shows that their properties are directed by temperature and by the size of the involved cations:

(1) Very interesting results concerning di-, and tritungstate structures are available. The most important works were proposed by Klevtsov *et al.* (6) and Nasseau *et al.* (7):

• Di-tungstates $AL(WO_4)_2$ can be listed into 20 structural groups born of 4 major families. It is possible to go from a structure to the others through slight structural modifications initiated either by temperature or by the cations size (Fig. 1a). In addition to these structural changes, the W^{6+} coordination number remains 6 or changes from 6 to 4.

• Concerning tritungstates, $L_2(WO_4)_3$, three structures are observed dependent on temperature and on the cations' ionic radius. At room temperature, if the L size is lower than that of Er^{3+}, L^{3+} cations are 6-fold coordinated. Over Er^{3+}, a structural change is observed (loss of symmetry) and L is then 8-fold coordinated.

(2) Similar structural synthesis can be made for monotungstates DWO_4, if we consider the structures of some of them. As seen in Fig. 1b, when the D ionic radius is higher than 1 Å, the compound has a scheelite structure (D 8-fold coordinated). When it is lower than 1 Å, the structure is wolframite-like (D 6-fold coordinated). Once again it looks like the structural changes are continuous and highly close to the cation size.

For 10 years, tungstates' vibrational properties have extensively been studied (8–12). Thanks to factor group analysis (FGA), it follows that Raman and IR spectra are easily understood and explained for all tungstate compounds. When free, WO_4^{2-} ions exhibit four vibrational modes called v_1(A1), v_2(E), v_3(F1), and v_4(F2). When these ions are included in a crystallographic network, the vibrational properties of the W–O bonds are dependant on the nature of the other elements involved in the network. In most cases, the highest frequency mode, useful for Raman shifter applications, corresponds to the symmetrical stretching of $[WO_x]$ polyhedra where $x = 4$ or 6. This mode is generally called v_1(A1) for tetrahedra. In the case of octahedra, all

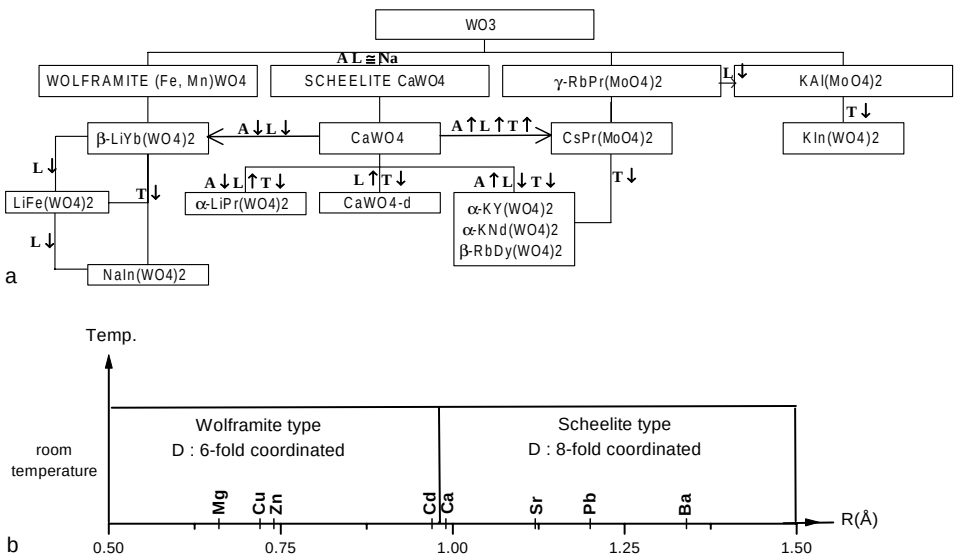

FIG. 1. (a) Structural relations in the double tungstates $AL(WO_4)_2$ family. (b) Structural evolution of monotungstates DWO_4 as a function of the D ionic radius.

W–O bonds are not equivalent (13) (some are terminal W–O bonds, others are involved in bridges) and will induce distinctly different vibration modes. The highest frequency Raman bands taken into account in this study correspond to the symmetrical stretching of W–O terminal bonds called ν_s(W–O). In a first approach, these bands and those of tetrahedra (ν_1) will be called, in a general way, ν_s.

RESULTS AND DISCUSSION

Table 1 gives the values of the highest intensity Raman band (ν_s) of each studied material, as well as other values taken from the literature. Figure 2 shows some of the Raman spectra obtained during this study. In a general way, for compounds in which tungsten atoms fill two different sites and for which two distinct ν_s bands are observed, only the most shifted one was taken into account in this study. This is mainly the case with some tritungstates such as $Gd_2(WO_4)_3$ in Fig. 2.

As can be seen, an evolution of tungstate Raman properties is observed, concerning both the ν_s band frequency and its integral. As said previously, tungstates' structural properties change regularly and continuously with the size of L cations. Correlations between Raman properties and physical chemistry parameters such as ionic radii have been searched. In this paper, calculations and a semiempirical approach are developed for the case of tritungstates $L_2(WO_4)_3$. The results obtained with this family of compounds can be fully transposed to the other for which only the major results are proposed.

1. Relationship between Structural and Raman Properties

1.1. *Band frequency evolution.* The Raman shift evolution of these materials has three major possible origins: the tungsten–oxygen bond lengths, the covalency degree, and the force constants.

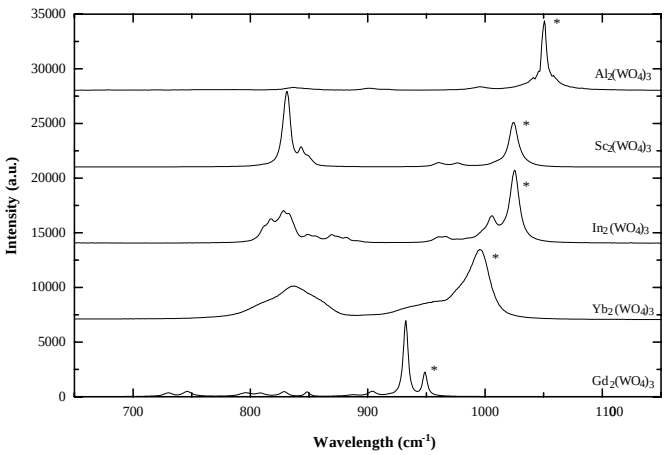

FIG. 2. Raman spectra of some studied tritungstates $L_2(WO_4)_3$. ν_1 are signaled with an asterisk.

TABLE 2
Theoretical (d_{theo}) and Average Observed (d_{obs}) Interatomic Distances of Tritungstates

			L^{3+}		$-O^{2-}$		$-W^{6+}$	
	Coord.	$r_{ion.}$	d_{theo} (Å)	d_{obs} (Å)	d_{theo} (Å)	d_{obs} (Å)	$E(\nu_1)$ (cm^{-1})
Al^{3+} (19)	6	0.53	1.89	1.83	1.92	1.78	1049
Sc^{3+} (20)	6	0.74	2.10	2.06	1.92	1.76	1024
Lu^{3+}	6	0.86	2.22	2.21	1.92	1.76	1010
La^{3+} (21)	8	1.16	2.52	2.52	1.92	1.77	927 (22)

Note: Ionic radii from (17, 18). O^{2-} radius, 1.36 Å.

(1) Bond length influence can be evidenced through a structural analysis of some compounds. In Table 2 are reported the average observed and theoretical (ionic radii sums) distances of W–O and L–O bond lengths:

- The W–O lengths deduced from structural data are largely smaller than the ionic sums, expressing an important covalency degree in these bonds. Also, whatever the L cation is, the W–O average distance remains almost constant. From these considerations, it results that the Raman shift evolution cannot be directly related to the W–O bond length.
- When the L–O bonds are considered, the slight difference between measured and ionic distances also expresses a small covalency degree of these bonds. For the investigated tritungstates, this degree decreases continuously when L cation radii increase. At the same time, the Raman shift of these compounds decreases continuously.

Consequently, it can be expected to link the Raman shift evolution and the L–O bond ionocovalency degree. This was done by introducing the L polarizability (23, 24) defined by relation [1]. In a first approach, all L cations have been considered having a fixed formal charge equal to $+3$. The polarizability is then reduced to a function of the L ionic radius only (similar considerations can be applied to double tungstates):

$$P = \frac{z}{\alpha r^3} \cong \frac{1}{r^3}. \qquad [1]$$

Figure 3a gives the evolution of di- and tritungstates' Raman shift versus P: the vibration frequency changes continuously with P and tends toward limit values which correspond to a maximum for each family. The highest Raman shift is reached with $Al_2(WO_4)_3$ at 1049 cm^{-1}.

The strong correlation between these two properties is observed best in Fig. 3b where the (Raman shift/L^{3+} polarizability) ratio is plotted as a function of L and A radii.

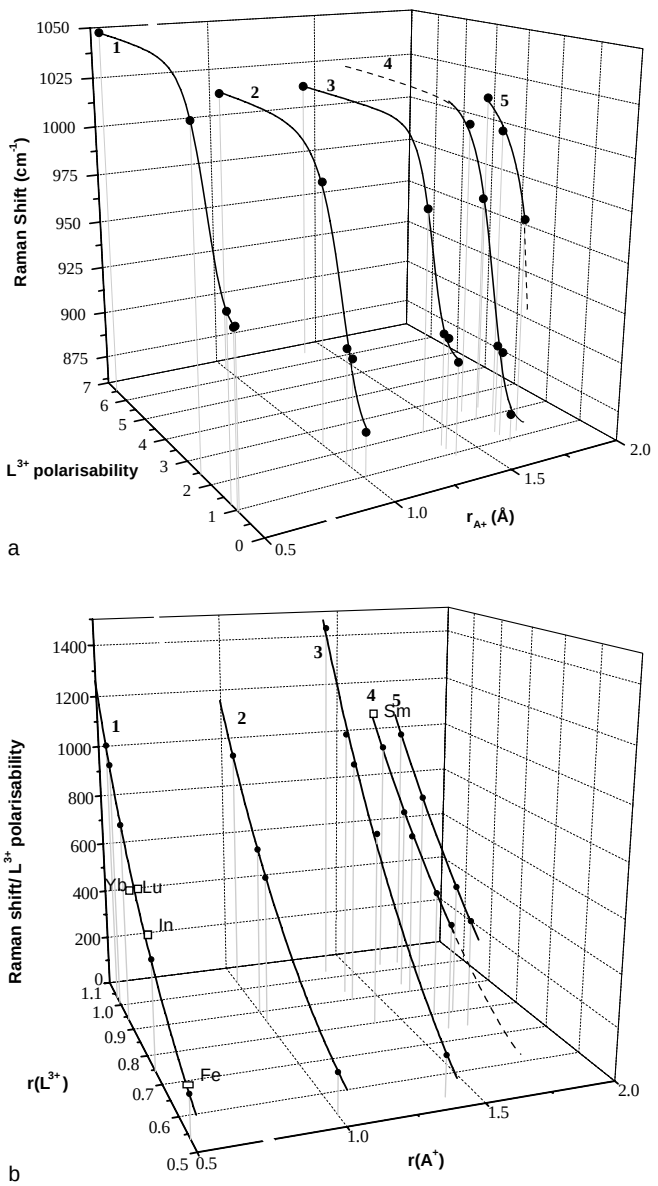

FIG. 3. (a) Correlation between tungstates ν_s frequency and L polarizability (P). (b) (Raman shift/P) versus R_{L3+} and R_{A+}; white squares, additionnal data in agreement with the correlation (cf. text). 1; $L_2(WO_4)_3$ 2; $LiL(WO_4)_2$; 3, $NaL(WO_4)_2$; 4, $KL(WO_4)_2$; 5, $RbL(WO_4)_2$.

Furthermore, this last figure can be used as a predictive tool to estimate any di- or tritungstate Raman shift. For instance, the measured value for europium tritungstate is 942 cm^{-1} (12) while the use of Fig. 2 gives 948 cm^{-1}. The difference between the two values is not negligible and is due to the calculation approximations. Nevertheless, in a qualitative way, this result gives a real physical meaning to this correlation. Other values taken from the literature also confirm this correlation: in addition to $Eu_2(WO_4)_3$ mentionned above, $Fe_2(WO_4)_3$ ($r_{Fe} = 0.55$ Å, $\nu_s = 1026\ cm^{-1}$ (25) and $KSm(WO_4)_2$ ($r_{Sm} = 1.079$ Å, $\nu_s = 899\ cm^{-1}$ (10)) were plotted in Fig. 3b with good agreement.

In the case of monotungstates DWO_4 where D is a divalent cation, it is difficult to correlate properties of D cations such as alkaline earths (Ca to Ba) or such as Pb, Zn, or Cd which present an $(n-1)d$ electronic layer. Recently, other different approaches have been unsuccessfully proposed (26).

(2) In order to evaluate the influence of the WO bond ionocovalency degree on the Raman properties, partial charge calculations were carried out using the Sanderson (27) model revised by Henry (28). This model is based on electronegativities equalization from which partial charges can be estimated using relation [2],

$$\delta_i = S_i(\bar{\chi} - \chi_i) = \frac{(\bar{\chi} - \chi_i)}{k\sqrt{\chi_i}}, \qquad [2]$$

where k is a constant, S_i is the softness of the i element, χ_i is its electronegativity expressed in Allred-Roschow's scale, and $\bar{\chi}$ is the average electronegativity of the whole compound or complex ions constituted of all i elements. It is called "well-balanced electronegativity of the chemical group" and is given by relation [3],

$$\chi = \frac{\sum_{i=1}^{n} P_i\sqrt{\chi_i} + kz}{\sum_{i=1}^{n} P_i/\sqrt{\chi_i}}, \qquad [3]$$

where z is the charge of the chemical group and P_i the stoichiometric coefficient of the i atom in the considered group.

Two mechanisms corresponding to the formation of a neutral tungstate molecule were considered.

- The first concerns the reaction between three tungsten cations and two LO_6 anions. It leads one to consider charge repartition around the W–O bonds. Results are proposed in Fig. 4a and show a charge evolution that is almost constant through the whole tritungstate family. This result is consistent with a constant W–O bond length and the W–O bond covalency degree has thus an inconsiderable influence on the Raman shift evolution.
- The second mechanism deals with the reaction between two L cations and three tungstate anions (WO_4). This corresponds to the study of charges repartition around the LO bonds. Results (Fig. 4b) show an evolution of partial charge and thus of the LO ionocovalency degree.

The correlation in Fig. 3 is not improved by the use of these calculated charges in relation [1]. Raman shift evolution is thus more influenced by the L size than by its charge.

To conclude, neither the W–O length nor the W–O covalency degree has an influence on the Raman frequency. Thus, only a variation of the W–O force constants can be responsible for its evolution, and this variation is induced by the nature of the L cation: covalent bonding is an oriented bonding and when the L size changes, the LO bond

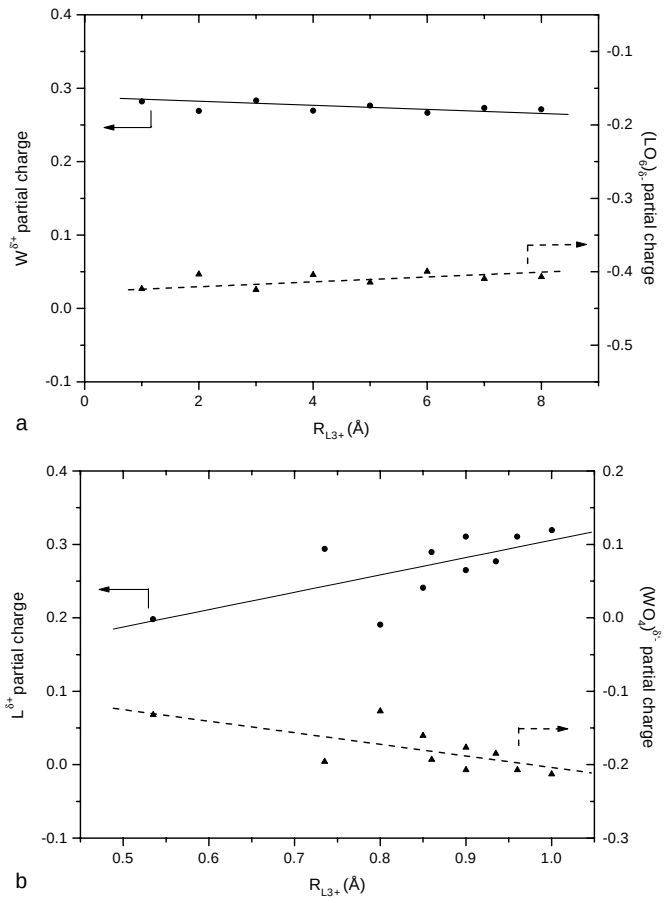

FIG. 4. Partial charge calculations for {W and (LO_6) ions} (a) and {L and (WO_4) ions} (b) in $L_2(WO_4)_3$.

covalency changes too and leads to a general rigidification of the structure which affects all other bond properties. Thus, the W–O force constant variation is a second-order consequence of the L cation, especially of its size.

1.2. *Band width and band intensity*. In almost all cases, Raman band broadening is mainly due to the interatomic potential anharmonicity (and eventually to crystal defects and/or size). As a consequence of the introduction of quantum terms it is not possible to relate it to simple physicochemical parameters as has been previously done for the frequency shift. We nevertheless have to consider that there are two cases that allow the relation between structural parameters and band width:

- If polyhedra are randomly distorted (each polyhedron having a specific conformation and then vibrating at a specific wavelength), the band broadening could be related to the polyhedra distortion as measured by Robinson *et al.* (29).
- If W atoms fill different symmetry sites there are as many vibrational band as there are site symmetries and then, once again, the band width can be related to structural parameters.

But these cases are particular ones and cannot be easily applied in the generalized approach we are developing herein.

Concerning the intensity of Raman scattering, it is a function of many terms where some of them have a quantic mechanic origin (energy difference between excited vibrational states, etc.). So once more, it cannot be linked to simple parameters such as ionic radii, etc.

2. *Tungstate Application Potential in Third-Order Nonlinear Optics*

The use of tungstate compounds in third-order nonlinear optics is dependent on two essential parameters: the Raman frequency shift and the Raman gain (frequency conversion efficiency). It is known that the Raman gain g of the probe Stokes beam at the wavelength λ_s is given by Eq. [4] (30):

$$g = \frac{2\lambda_p \lambda_s^2}{hcn_s^2} \frac{N}{\Omega} \left(\frac{d\sigma_{sp}^R}{d\omega}\right), \qquad [4]$$

where λ_p is the pump laser wavelength, c is the light celerity, h is Planck's constant, n_s is the spontaneous Raman scattering quantum number, N is the total number of scattering centers per unit volume, Ω is the band width for which the intensity is half of the maximum intensity, and σ_{sp}^R is the spontaneous Raman scattering cross section per unit volume for Stokes scattering. In practice σ_{sp}^R is not measured but instead the differential cross section per unit volume ($d\sigma_{sp}^R/d\omega$), where $d\omega$ means an elementary solid angle. Such a parameter is very useful since the spontaneous Raman scattering intensity I_{sp}^R is given by $k(d\sigma_{sp}^R/d\omega)$.

Then, g can be expressed by

$$g = \frac{2\lambda_p \lambda_s^2}{hcn_s^2} \frac{N}{k} \frac{I_{sp}^R}{\Omega} \propto \Sigma. \qquad [5]$$

Thus, the ratio $\Sigma = (I_{sp}^R/\Omega)$ appears as a valuable parameter to compare the Stokes Raman frequency conversion efficiency of tungstates.

Actually, barium nitrate is the reference of third-order nonlinear materials. If this Σ ratio is taken as a reference, it will be possible to estimate any tungstate application power through the use of a normalized Σ given by the $\Sigma_{tungstate}/\Sigma_{barium\ nitrate}$ ratio (Table 3).

In Fig. 5, tungstate' Raman shift is represented versus the normalized Σ. From this figure it is easy to quickly estimate tungstates having a high-frequency shift (e.g., $Al_2(WO_4)_3$) and tungstates having a high conversion efficiency (high Σ) (e.g., β-RbGd$(WO_4)_2$).

Another interest in such a representation is the possibility to adapt the choice of the Raman shifter with the laser pump wavelength for a given application.

TABLE 3
Comparison of the v_s Band Integral of Some Tungstates with That of Barium Nitrate

Compound	Function	w (cm^{-1})	A	I	Ω (cm^{-1})	Σ	$\Sigma/\Sigma_{Ba(NO3)2}$
$Ba(NO_3)_2$	Gauss	2.5	15635	15635	2.5	6254	1
$Al_2(WO_4)_3$	Lorentz	11.6	55087	3023	11.6	261	0.04
$Gd_2(WO_4)_3$ (1)	Lorentz	5.45	55577	6492	5.45	1191	0.19
$Gd_2(WO_4)_3$ (2)	Lorentz	5.14	167328	20724	5.14	4032	0.64
$KY(WO_4)_2$	Lorentz	6.87	191732	17767	6.87	2586	0.41
$KGd(WO_4)_2$	Lorentz	6.99	395216	35994	6.99	5149	0.82
$KSc(WO_4)_2$	Lorentz	6.08	72892	7632	6.08	1255	0.20
$RbSc(WO_4)_2$	Lorentz	6.06	89305	9381	6.06	1548	0.25
α-$RbGd(WO_4)_2$	Lorentz	9.40	170078	11519	9.40	1225	0.20
β-$RbGd(WO_4)_2$	Gauss	2.72	33470	33470	2.72	12305	1.96
$KBi(WO_4)_2$	Lorentz	5.40	64969	7659	5.40	1418	0.23
$LiGd(WO_4)_2$	m-Lorentz	16.39	660822	25667	16.39	1566	0.25
$NaGd(WO_4)_2$	m-Lorentz	16.11	146282	5781	16.11	359	0.06
$NaY(WO_4)_2$	m-Lorentz	16.29	272376	10644	16.29	653	0.10

Functions:

Lorentz, $y = y_0 + \frac{2A}{\pi}\frac{w}{4(x - xc)^2 + w^2} \rightarrow I = \frac{2A}{\pi w}, \quad \Omega = w;$

Gauss, $y = y_0 + Ae^{-(x-xc)^2/2W^2} \rightarrow I = A \qquad \Omega = w.$

Due to the large range of available pump sources (laser and laser diodes) all of these compounds present great interest for frequencies generation based on crystals using third-order nonlinear optical techniques.

CONCLUSIONS AND PERSPECTIVES

In order to understand tungstates' Raman behavior and to rationalize the search for new efficient nonlinear optical materials, a comprehensive study of their Raman shift properties was carried out.

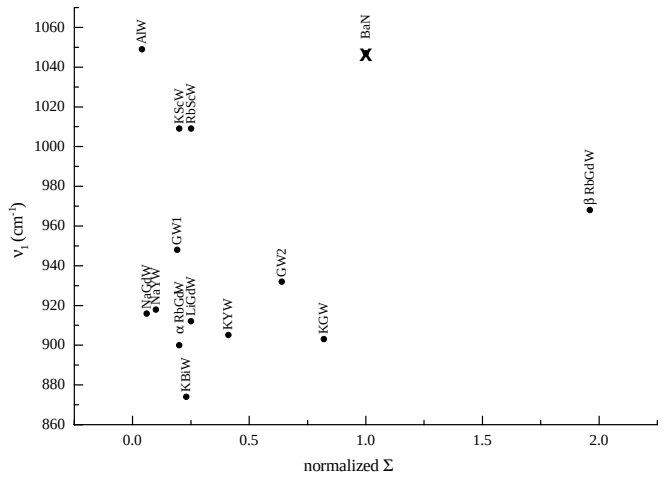

FIG. 5. Figure of merit of tungstates for application in third-order nonlinear optics where v_s (in cm^{-1}) is the symmetrical streching of [WO_x] polyhedra frequency and Σ is the normalized ratio $\Sigma_{tungstate}/\Sigma_{barium\ nitrate}$.

• Concerning di- and tritungstates, the Raman shift frequency (v_s, symmetric stretching of WO_x polyedra) is directly and essentially influenced by the nature of the trivalent cation involved in these compounds. The size of the trivalent cation has an indirect consequence on W–O force constants. This influence was shown to be continuous and allows the prediction of any tungstate Raman shift frequency.

• A figure of merit expressing the v_s of the W–O terminal bond's frequency as a function of the Raman gain for the three investigated tungstate families has been proposed. It allows one to quickly find and adapt Raman shifter materials with pump sources for a given application.

To go further, thanks to this study, we have shown that the search for new efficient materials should be oriented toward compounds such as β-$RbGd(WO_4)_2$ (or similar compounds having the same structure) which could be of high interest for laser applications thanks to their high-frequency conversion efficiency.

Finally, this approach is not exclusive to tungstate compounds and could be applied to any other chemical family, for instance, molybdates which are also good Raman shifters. It would lead to a fast overview of their application possibilities as well.

REFERENCES

1. P. G. Zverev, J. T. Murray, R. C. Powell, and T. T. Basiev, *Opt. Commun.* **97,** 59 (1993).
2. A. A. Kaminskii, "Laser and Optical Science and technology series," CRC, Boca Raton, FL, 1996.

3. A. A. Kaminskii, H. Nishioka, Y. Kubota, K. Ueda, H. Takuma, S. N. Bagaev, and A. A. Pavliuk, *Phys. Stat. Sol.* (*a*), **148,** 619 (1995).
4. F. D. Hardcastle and I. E. Wachs, *J Raman Spectrosc.* **26,** 397 (1995).
5. W. B. White, *in* "Infrared and Raman spectroscopy of Lunar and Terrestrial Minerals" (C. Karr, Jr., Ed.), Academic Press, New York, 1975.
6. P. V. Klevtsov and R. F. Klevtsova, *J. Struct. Chem.* **18-3,** 419 (1977).
7. K. Nasseau, J. W. Shiever, and E. T. Keve, *J. Solid State Chem.* **3,** 411 (1971).
8. J. Hanuza, M. Maczka, K. Hermanowicz, M. Andruszkiewicz, A. Pietrasko, W. Strek, and P. Deren, *J. Solid State Chem.* **105,** 49 (1993).
9. J. Hanuza, M. Maczka, and J. H. Van Der Maas, *J. Solid State Chem.* **117,** 177 (1995).
10. M. Maczka, *J. Solid State Chem.* **129,** 287 (1997).
11. J. Hanuza and L. Macalik, *Spectrochim. Acta* **43A-3,** 361 (1987).
12. V. I. Tsaryuk, V. F. Zolin, and B. F. Dzhurinskii, *Russ. J. Inorg. Chem.* **41-1**, 150 (1996).
13. J. Hanuza, L. Macalik, M. Maczka, E. T. G Lutz, and J. H. Van Der Maas, *J. Mol. Struct.* **511–512,** 85 (1999).
14. E. Gallucci, C. Goutaudier, G. Boulon, M.Th.Cohen-Adad, and B. F. Mentzen, *J. Crystal Growth* **65,** 895 (2000).
15. E. Gallucci, C. Goutaudier, M. Th. Cohen-Adad, B. F. Mentzen, and T. Hansen, *J. Alloys Compds.* **306,** 227 (2000).
16. E. Gallucci, Tungstates pour la conversion de fréquences laser par décalage Raman. Relation propriétés structurales/propriétés vibratoires, croissance cristalline et caractérisations. Thèse 243–2000, Université Claude Bernard Lyon I, France, 2000
17. R. D. Shannon, *Acta Crystallogr. A* **32,** 751 (1976).
18. Y. Q. Jia, *J. Solid State Chem.* **95,** 184 (1991).
19. D. C. Craig and N. C. Stephenson, *Acta Crystallogr. B* **24,** 1250 (1968).
20. S. C. Abrahams and J. L. Bernstein, *J. Chem. Phys.* **45-8,** 2745 (1966).
21. M. Gärtner, D. Abeln, A. Pring, M. Wilde, and A. Reller, *J. Solid State Chem.* **111,** 128 (1994).
22. L. J. Burcham and I. E. Wachs, *Spectrochim. Acta*, *A* **54,** 1355 (1998).
23. K. Fajans, *Naturwissenschaften* **11,** 165 (1923).
24. K. Fajans, *Struct. Bonding* (*Berlin*) **3,** 88 (1967).
25. J. A. Horsley, I. E. Wachs, J. M. Brown, G. H. Via, and Hardcastle F. D., *J. Phys. Chem.* **91,** 4014–4020 (1987).
26. T. T. Basiev, A. A. Sobol, Y. K. Voronko, and P. G. Zverev, *Opt. Mater.* **15,** 205 (2000).
27. R. T. Sanderson, "Inorganic Chemistry." Reinhold, New York, 1967.
28. M. Henry, Application du concept d'électronégativité aux processus d'hydrolyse et de condensation en chimie minérale, Thèse, Université Pierre et Marie Curie, Paris, France, 1988.
29. K. Robinson, G. V. Gibbs, and P. H. Ribbe, *Science* **172,** 172 (1971).
30. J. Y. Courtois, Optique non linéaire, *in* "Les Laser," (C. Fabre and J. P. Pocholle, Eds.), p. 87, Les Editions de Physique Publishers, 1996.